The Electrochemical Society
Advancing solid state & electrochemical science & technology

The Electrochemical Society
Advancing solid state & electrochemical science & technology

Communication—Oscillating Oxygen Concentration Transport through PEM Fuel Cell Gas Diffusion Layer: Variation of the Phase Angle

To cite this article: Andrei Kulikovsky 2024 *ECS Adv.* **3** 024503

ECS Advances, 2024 **3** 024503

Communication—Oscillating Oxygen Concentration Transport through PEM Fuel Cell Gas Diffusion Layer: Variation of the Phase Angle

Andrei Kulikovsky[*,a,z]

Forschungszentrum Jülich GmbH, Theory and Computation of Energy Materials (IEK–13), Institute of Energy and Climate Research, D–52425 Jülich, Germany

Recently, it was shown that performance of the cathode catalyst layer in PEM fuel cell dramatically improves if the oxygen concentration (OC) at the catalyst/ gas diffusion layer (GDL) interface oscillates in–phase with the overpotential. However, OC oscillations could only be organized in the cathode channel. Does transport through the GDL affect the phase angle of OC oscillations? Below, it is shown that at low frequencies below 1 Hz, the GDL does not change this phase angle. At high frequencies, the phase angle after transport through the GDL is $-3\pi/4$ regardless of the GDL parameters.

[DOI: 10.1149/2754-2734/ad3cf4]

Manuscript submitted December 30, 2023; revised manuscript received April 2, 2024. Published April 18, 2024.

Experiments of Kim et al.[1] and Hwang et al.[2] have revealed dramatic improvement of PEM fuel cell performance under oscillating velocity of the cathode channel flow. The authors explained the effect by improvement of oxygen transport through the porous layers thanks to the oscillating flow velocity. However, the mechanism of this improvement was not fully understood.

Recently, it has been shown that the oxygen concentration (OC) at the cathode catalyst layer (CCL) / gas diffusion layer (GDL) interface oscillating in–phase with the oxygen reduction reaction (ORR) overpotential dramatically decreases the CCL impedance.[3] Oscillating OC generates a sub–layer in the CCL, where oxygen transport is fast and the ORR rate is high. Working as an ideal non–polarizable electrode, this sub–layer dramatically reduces the CCL impedance.[3]

Technically, direct supply of oscillating OC at the CCL/GDL interface is not feasible. However, oscillating OC can be organized in the cathode channel by applying harmonic perturbation of pressure at the channel inlet. This raises the problem of phase shift introduced by the GDL. In other words, the question is what would be the phase shift of OC oscillations at the CCL/GDL interface with respect to OC oscillations in the channel? The simple model below aims to clarify the problem. To the best of our knowledge, so far, the GDL phase properties for oxygen transport have not been studied in fuel cell literature.

Model

Schematic of the PEMFC cathode side is shown in Fig. 1. To study oxygen transport through the GDL, we will employ the simplest model for the cathode catalyst layer attached. The electrode model is based on the following basic assumptions:

- The CCL proton conductivity and oxygen diffisivity are large, hence variation of the static η^0, c^0 and perturbed η^1, c^1 overpotential and oxygen concentration through the CCL depth is negligible.

Strictly speaking, this assumption means that the model and results below are valid provided that the cell current density is small, typically below 100 mA cm^{-2}. The high–current regime requires numerical calculations; this regime will be considered in a full–length paper. However, we can expect that the model of electrode attached to the GDL does not change much the phase properties of the oxygen transport in the GDL, which is described by Eq. 1 regardless of the cell current:

$$\frac{\partial c_b}{\partial t} - D_b \frac{\partial^2 c_b}{\partial x^2} = 0 \qquad [1]$$

where D_b is the GDL oxygen diffusivity, x is the coordinate through the cell counted from the membrane (Fig. 1).

To relate oxygen flux in the GDL and the ORR overpotential we need proton charge conservation equation in the CCL. Due to fast proton and oxygen transport through the CCL, the charge conservation reads

$$C_{dl} l_t \frac{\partial \eta_0}{\partial t} - j_0 = -i_* l_t \left(\frac{c_1}{c_{ref}}\right) \exp\left(\frac{\eta}{b}\right) \qquad [2]$$

Here, C_{dl} is the volumetric double layer capacitance, η_0 is the positive by convention ORR overpotential, j_0 is the cell current density, i_* is the volumetric ORR exchange current density, l_t is the CCL thickness, c_1 is the OC at the CCL/GDL interface, c_{ref} is the reference OC, b is the ORR Tafel slope.

Using the dimensionless variables

$$\tilde{x} = \frac{x}{l_t}, \quad \tilde{t} = \frac{t i_*}{C_{dl} b}, \quad \tilde{c} = \frac{c}{c_{ref}}, \quad \tilde{\eta} = \frac{\eta}{b}, \quad \tilde{j} = \frac{j}{i_* l_t},$$
$$\tilde{D}_b = \frac{4F D_b c_{ref}}{i_* l_t^2}, \quad \tilde{\omega} = \frac{\omega C_{dl} b}{i_*}, \qquad [3]$$

where $\tilde{\omega}$ is the angular frequency of applied AC signal, Eqs. 1, 2 take the form

$$\mu^2 \frac{\partial \tilde{c}_b}{\partial \tilde{t}} - \tilde{D}_b \frac{\partial^2 \tilde{c}_b}{\partial \tilde{x}^2} = 0, \quad \mu \equiv \sqrt{\frac{4F c_{ref}}{C_{dl} b}}, \qquad [4]$$

$$\frac{\partial \tilde{\eta}_0}{\partial \tilde{t}} - \tilde{j}_0 = -\tilde{c}_1 \exp \tilde{\eta}_0 \qquad [5]$$

Linearization and Fourier–transform of Eqs. 4, 5 is performed using Eqs. 6:

$$\begin{aligned}
\tilde{c}_b(\tilde{x}, \tilde{t}) &= \tilde{c}_b^0(\tilde{x}) + \tilde{c}_b^1(\tilde{x}, \tilde{\omega})\exp(\mathrm{i}\tilde{\omega}\tilde{t}), \quad |\tilde{c}_b^1| \ll \tilde{c}_b^0 \\
\tilde{c}(\tilde{t}) &= \tilde{c}^0 + \tilde{c}^1(\tilde{\omega})\exp(\mathrm{i}\tilde{\omega}\tilde{t}), \quad |\tilde{c}^1| \ll \tilde{c}^0 \\
\tilde{j}(\tilde{t}) &= \tilde{j}^0 + \tilde{j}^1(\tilde{\omega})\exp(\mathrm{i}\tilde{\omega}\tilde{t}), \quad |\tilde{j}^1| \ll \tilde{j}^0 \\
\tilde{\eta}(\tilde{t}) &= \tilde{\eta}^0 + \tilde{\eta}^1(\tilde{\omega})\exp(\mathrm{i}\tilde{\omega}\tilde{t}), \quad |\tilde{\eta}^1| \ll \tilde{\eta}^0
\end{aligned} \qquad [6]$$

where the subscripts 0 and 1 mark the static shapes and the small perturbation amplitudes in the ω–space. Substituting Eqs. 6 into

---

[*] Electrochemical Society Member.

[a] Also at: Lomonosov Moscow State University, Research Computing Center, 119991 Moscow, Russia.

[z] E-mail: A.Kulikovsky@fz-juelich.de

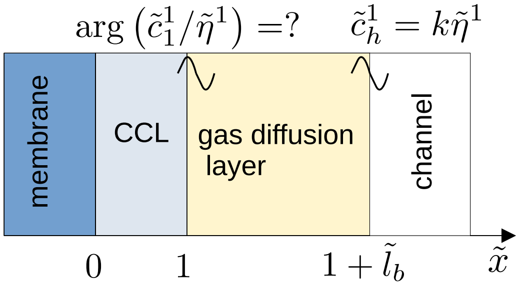

Figure 1. Schematic of the oxygen transport layer (GDL) placed between the cathode catalyst layer (CCL) and the cathode channel. $\tilde c_1^1$ and $\tilde c_h^1$ are the dimensionless oxygen concentration perturbation amplitudes on either side of the GDL; the phase shift between the two is a subject of this paper.

Eqs. 4, 5, neglecting terms with the perturbations product and subtracting the respective static equations, we come to the linear Eqs. relating the small perturbation amplitudes $\tilde\eta^1(\tilde\omega)$, $\tilde j^1(\tilde\omega)$, and $\tilde c_b^1(\tilde\omega, \tilde x)$:

$$\tilde D_b \frac{\partial^2 \tilde c_b^1}{\partial \tilde x^2} = \mathrm{i}\tilde\omega\mu^2\tilde c_b^1, \quad \tilde D_b \left.\frac{\partial \tilde c_b^1}{\partial \tilde x}\right|_{\tilde x=1} = \tilde j^1, \quad \tilde c_b^1(1+\tilde l_b) = k\tilde\eta^1 \qquad [7]$$

$$\tilde j^1 = \mathrm{i}\tilde\omega\tilde\eta^1 + \tilde j_0\left(\frac{\tilde c_1^1}{\tilde c_1^0} + \tilde\eta^1\right) \qquad [8]$$

where the static Tafel law

$$\tilde j_0 = \tilde c_1^0 \mathrm{e}^{\tilde\eta^0} \qquad [9]$$

was used to eliminate $\mathrm{e}^{\tilde\eta^0}$ from Eq. 8. The amplitude factor $k > 0$ in Eq. 7 is real and hence the right boundary condition for Eq. 7 means that applied in the channel OC perturbation varies in–phase with the overpotential. Simultaneous in–phase oscillations of the oxygen concentration and overpotential applied at the CCL/GDL interface has been a key assumption in Ref. 3. Here, we show what happens to the OC phase if this boundary condition is applied at the channel/GDL interface.

Solving Eq. 7 and setting $\tilde x = 1$ in the solution we get

$$\tilde c_b^1(1) = -\frac{\tilde j^1 \tanh(q\tilde l_b)}{q\tilde D_b} + \frac{k\tilde\eta^1}{\cosh(q\tilde l_b)}, \quad q \equiv \mu\sqrt{\mathrm{i}\tilde\omega/\tilde D_b} \qquad [10]$$

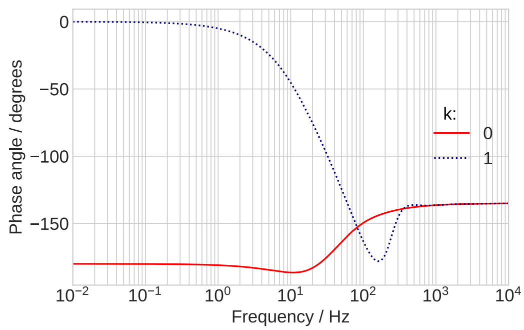

Figure 2. The phase angle between the oxygen concentration perturbation $\tilde c_1^1$ at the CCL/GDL interface and the applied perturbation $\tilde\eta^1$ for the indicated values of parameter k. $k = 0$: no applied perturbation of the OC in channel. $k = 1$: the dimensionless perturbation amplitudes of applied in channel OC and overpotential are equal. The other parameters are listed in Table I.

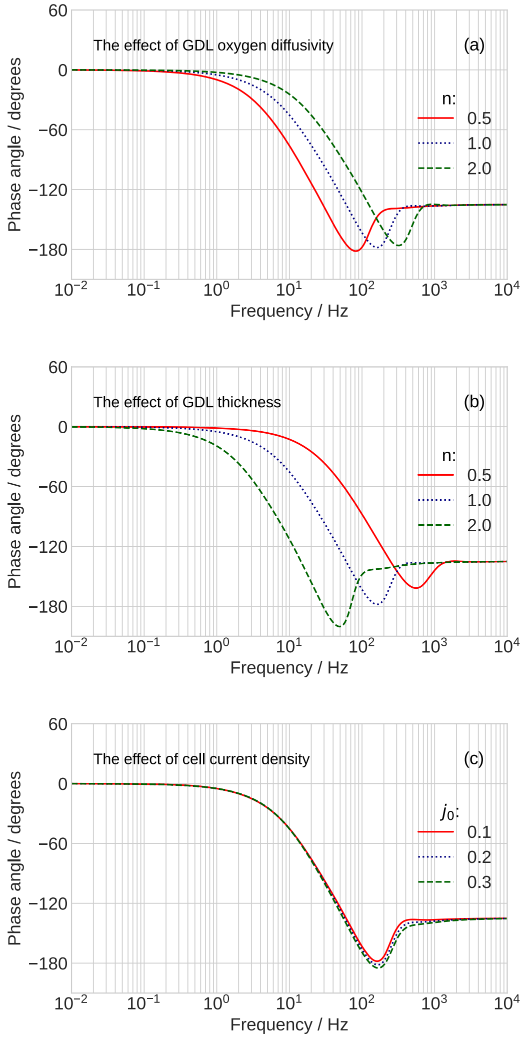

Figure 3. The effect of (a) the GDL oxygen diffusivity D_b, (b) the GDL thickness l_b, and (c) the cell current density j_0 (A cm^{-2}) on the phase angle between the oxygen concentration $\tilde c_1^1$ at the CCL/GDL interface and applied $\tilde\eta^1$. In (a), (b) indicated are the factors n by which the base–case parameter value (Table I) is multiplied. All the curves are calculated with k=1.

Continuity of the OC at the CCL/GDL interface means that $\tilde c_b^1(1) = \tilde c_1^1$. Using this equation and eliminating $\tilde j_1$ from Eqs. 10 and 8, we get the ratio of the OC perturbation $\tilde c_1^1$ at the CCL/GDL interface to the overpotential perturbation $\tilde\eta^1$:

$$G \equiv \frac{\tilde c_1^1}{\tilde\eta^1} = \frac{kq\tilde D_b - (\tilde j_0 + \mathrm{i}\tilde\omega)\sinh(q\tilde l_b)}{q\tilde D_b\cosh(q\tilde l_b) + \tilde j_0\sinh(q\tilde l_b)/\tilde c_1^0}. \qquad [11]$$

Our main interest is the phase angle of the function G, Eq. 11. Since oxygen concentration in the channel oscillates in–phase with the overpotential, the phase angle $\arg(G)$ is the phase shift acquired by the OC oscillations upon transport through the GDL.

Results and Discussion

Analytical expression for $\arg(G)$ is rather cumbersome and below, we show numerical results for the frequency dependence of $\arg(G)$ (Fig. 2). The parameters used for calculations are listed in Table I. With $k = 0$ (no applied OC perturbation), a large phase shift between $\tilde c_1^1$ and $\tilde\eta^1$ exists in the whole frequency range due to oxygen transport through the GDL (red curve in Fig. 2). However, with $k = 1$, for the frequencies below 1 Hz, the phase shift vanishes and the OC $\tilde c_1^1$ at the CCL/GDL interface oscillates in–phase with the overpotential (dotted blue curve in Fig. 2).

The effect of GDL oxygen diffusivity D_b and thickness l_b on the phase angle $\arg(G)$ is shown in Figs. 3a, b. As expected, the

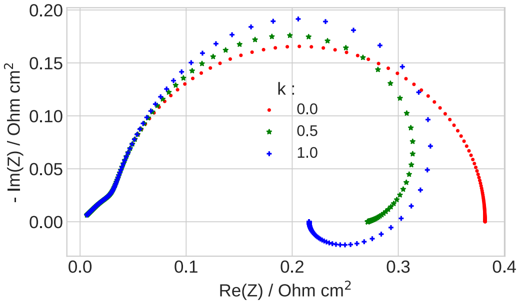

Figure 4. Nyquist spectra of the system CCL + GDL calculated using the analytical model.[5] The oxygen concentration in the channel varies proportionally to the ORR overpotential; the values of parameter k, Eq. 7, are indicated. The air flow stoichiometry is assumed to be infinite.

Table I. The typical PEM fuel cell parameters used in calculations. The parameters correspond to a standard PEM fuel cell with the CCL thickness of 10 μm and Sigracet 25 BC GDL; the transport coefficients have been measured using impedance spectroscopy.[4] The Tafel slope of 30 mVexp corresponds to 30 · 2.303 ≃ 70 mV/decade.

Tafel slope b, mV/exp	30
Double layer capacitance C_{dl}, F cm^{-3}	20
ORR Exchange current density i_*, A cm^{-3}	10^{-3}
Oxygen diffusion coefficient in the GDL, D_b, cm^2 s^{-1}	0.02
GDL thickness l_b, cm	$230 \cdot 10^{-4}$
Catalyst layer thickness l_t, cm	$10 \cdot 10^{-4}$
Cell temperature T, K	273 + 80
Cathode pressure, bar	1
Cell current density j_0, A cm^{-2}	0.1

frequency range where GDL is "transparent" to OC phase angle increases with the growth of D_b (Fig. 3a) and with the decrease of l_b (Fig. 3b). Note that the effect of l_b is stronger: twice lower l_b increases the upper frequency where $\arg(G) \simeq 0$ by an order of magnitude (cf. green and red curves in Fig. 3b). Figure 3c shows the effect of cell current density on the phase shift. As can be seen, this effect is marginal: variation of the cell current in the range of 0.1 to 0.3 A cm^{-2} practically does not alter the GDL phase transparency "window" on the frequency scale. All the curves in Figure 3 are calculated with the amplitude factor k=1.

Figure 4 shows the impedance spectra of the system "CCL + GDL" calculated using the exact low–current analytical solution for the PEMFC impedance[5] for the three indicated values of parameter k. As can be seen, oscillations of oxygen concentration in the channel applied in–phase with the ORR overpotential (see the right boundary condition for Eq. 7) dramatically reduce the low––frequency system impedance. At higher frequencies, the impedance modulus increases due to non–zero phase angle of the OC oscillations acquired upon transport through the GDL. Note that the model[5] takes into account variation of perturbation amplitudes through the CCL depth, which is ignored above.

Last but not least, it can be shown analytically that as the frequency tends to infinity, the phase angle of OC oscillations transported through the GDL tends to the universal constant $\phi_{\lim}$

$$\phi_{\lim} = \lim_{\tilde{\omega}\to\infty} \arg\left(G(\tilde{\omega})\right) = -\frac{3\pi}{4}, \qquad [12]$$

or −135 degrees (Figs. 3a, 3b). In other words, after passing through the GDL, the phase of any sufficiently high–frequency OC oscillations is $-3\pi/4$, regardless of the GDL transport properties. Note that the transition frequency to this limiting phase depends on the GDL thickness and diffusivity, e.g. the lower the thickness, the higher the transition frequency (Fig. 3b).

To summarize, zero phase shift introduced by the GDL upon transport of low–frequency oxygen concentration oscillations makes it possible to arrange a much more efficient regime of PEM fuel cell operation. GDL in PEMFCs is usually optimized in terms of static oxygen transport resistivity. The analysis above shows that equally important are the GDL phase properties. More details on the effect demonstrated in Fig. 4 will be published in a full–length paper.

ORCID

Andrei Kulikovsky https://orcid.org/0000-0003-1319-576X

References

1. Y. H. Kim, H. S. Han, S. Y. Kim, and G. H. Rhee, "Influence of cathode flow pulsation on performance of proton-exchange membrane fuel cell." *J. Power Sources*, **185**, 112 (2008).
2. Y.-S. Hwang, D.-Y. Lee, J. W. Choi, S.-Y. Kim, S. H. Cho, P. Joonho, M. S. Kim, J. H. Jang, S. H. Kim, and S.-W. Cha, "Enhanced diffusion in polymer electrolyte membrane fuel cells using oscillating flow." *Int. J. Hydrogen Energy*, **35**, 3676 (2010).
3. A. Kulikovsky, "Performance of a PEM fuel cell cathode catalyst layer under oscillating potential and oxygen supply." *Electrochem. Comm.*, **159**, 107655 (2024).
4. T. Reshetenko and A. Kulikovsky, "Variation of PEM fuel cell physical parameters with current: Impedance spectroscopy study." *J. Electrochem. Soc.*, **163**, F1100 (2016).
5. A. Kulikovsky, "Analytical impedance of PEM fuel cell cathode including oxygen transport in the channel, gas diffusion and catalyst layers." *J. Electrochem. Soc.*, **169**, 034527 (2022).